



ATTI
DELLA
SOCIETÀ TOSCANA
DI
SCIENZE NATURALI

MEMORIE • SERIE A • VOLUME CXXII • ANNO 2015



Edizioni ETS



Con il contributo del Museo di Storia Naturale dell'Università di Pisa



e della Fondazione Cassa di Risparmio di Lucca

INDICE - CONTENTS

<p>N. BEDOSTI, W. LANDINI, R. D'ANASTASIO – The increase of bony mass in a small Cyprinodontidae from the Messinian deposit of Monte Tondo (Ravenna, Italy); paleoecological implications <i>Incremento della massa ossea in un piccolo Cyprinodonteae proveniente dai depositi del Messiniano superiore di Monte Tondo (Ravenna, Italia): implicazioni paleoecologiche</i></p>	<p>pag. 5</p>	<p>F. RAPETTI – Dall'archivio meteorologico del Seminario arcivescovile Santa Caterina d'Alessandria di Pisa un contributo alla conoscenza della storia pluviometrica della città dall'inizio del Settecento ad oggi <i>From the meteorological archives of the Seminary of St. Catherine of Alexandria in Pisa a contribution to the knowledge of the pluviometric history of the city from the beginning of the Eighteenth century up to the present</i></p>	<p>» 63</p>
<p>A. CIAMPALINI, F. RASPINI, S. MORETTI – Landside back monitoring and forecasting by using PSInSAR: technique: the case of Naso (Sicily, southern Italy) <i>Analisi e previsione dei fenomeni franosi tramite l'utilizzo della tecnica PSInSAR: il caso di Naso (Sicilia, Italia Meridionale)</i></p>	<p>» 19</p>	<p>G. SARTI, V. ROSSI, S. GIACOMELLI – The Upper Pleistocene "Isola di Coltano Sands" (Arno coastal plain, Tuscany Italy): review of stratigraphic data and tectonic implications for the southern margin of the Viareggio basin <i>Le sabbie del Pleistocene superiore di Isola di Coltano (Pianura costiera dell'Arno, Toscana, Italia): revisione dei dati stratigrafici ed implicazioni tettoniche per il margine meridionale del bacino di Viareggio</i></p>	<p>» 75</p>
<p>S. FARINA, G. ZANCHETTA – On a bone breccia near Uliveto Terme (Monte Pisano, Italy) <i>Su una breccia ossifera nelle vicinanze di Uliveto Terme (Monte Pisano, Italia)</i></p>	<p>» 33</p>	<p>M. SERRADIMIGNI, M. COLOMBO – Ocra Rossa tra funzionalità e simbolismo: il caso del complesso litico dell'epigravettiano finale di Grotta Continenza (Trasacco-AQ) <i>Red ochre between functionality and symbolism: the case of the lithic assemblage of the Late Epigravettian in Grotta Continenza (Trasacco-AQ)</i></p>	<p>» 85</p>
<p>L. JASELLI – Virginio Caccia e il suo contributo alla conoscenza naturalistica del territorio di S. Colombano al Lambro <i>Virginio Caccia and his contribution to the naturalistic knowledge of the territory of S. Colombano al Lambro</i></p>	<p>» 37</p>	<p>Processi Verbali - http://www.stsn.it</p>	<p>» 97</p>
<p>M. LEZZERINI, M. TAMPONI – X-ray fluorescence analysis of trace elements in silicate rocks using fused glass discs <i>Analisi in fluorescenza a raggi X degli elementi in traccia in rocce silicatiche usando dischi di vetro fuso</i></p>	<p>» 45</p>		
<p>M. RAMACCIOTTI, M. SPAMPINATO, M. LEZZERINI. The building stones of the apsidal walls of the Pisa's Cathedral <i>Le pietre delle murature dell'abside del Duomo di Pisa</i></p>	<p>» 55</p>		

ANDREA CIAMPALINI (*), FEDERICO RASPINI (*), SANDRO MORETTI (*)

LANDSLIDE BACK MONITORING AND FORECASTING BY USING PSINSAR TECHNIQUE: THE CASE OF NASO (SICILY, SOUTHERN ITALY)

Abstract - *Landslide back monitoring and forecasting by using PSInSAR: technique: the case of Naso (Sicily, southern Italy).* The village of Naso (Sicily, southern Italy), for its peculiar geological setting, was affected by several landslide phenomena (rockfalls, complex landslides) during the first months of the 2010. The village is located on top of hard-brittle Quaternary deposits (calcareous sandstones), lying on a soft-plastic substratum. These phenomena represent a serious risk for the buildings stability and people safety. In order to study the slope instability evolution of this area, satellite Synthetic Aperture Radar (SAR) images, acquired during the last 20 years, have been processed and analyzed. These data have been acquired by using C-band and X-band sensors. Results highlighted that the 2010 events was preceded by several acceleration periods and that the slope is still affected by ground deformation.

Keywords - Remote sensing, landslide, Radar, Permanent Scatterer, back monitoring

Riassunto - *Analisi e previsione dei fenomeni franosi tramite l'utilizzo della tecnica PSInSAR: il caso di Naso (Sicilia, Italia Meridionale).* Il villaggio di Naso (Sicilia, Italia) a causa della sua particolare conformazione geologica è stato interessato da numerosi fenomeni franosi (crolli in roccia, frane complesse) durante i primi mesi del 2010. Il centro abitato è situato su un rilievo costituito da depositi quaternari consolidati a comportamento fragile che giacciono su di un substrato a comportamento plastico. I fenomeni che si sono verificati rappresentano un rischio elevato sia per la stabilità degli edifici che per la sicurezza degli abitanti. Al fine di studiare la deformazione dell'area di studio sono state acquisite le immagini satellitari (SAR) degli ultimi 20 anni. Tali immagini sono state processate ed analizzate in dettaglio. Le immagini radar sono state acquisite nelle bande C e X. I risultati hanno evidenziato che gli eventi del 2010 sono stati preceduti da periodi di accelerazione nella deformazione del terreno e che l'area è tuttora interessata da deformazioni consistenti.

Parole chiave - Telerilevamento, frane, Radar, Permanent Scatterer, monitoraggio

1. INTRODUCTION

Rockfalls and rockslides can represent very hazardous natural hazards which have high socio-economic and environmental impact on buildings, infrastructures and for people safety. These kinds of phenomena are usually fast but they can be preceded by a period of slow movements prior to slope failure. In Europe the presence of historical cities, characterized by a valu-

able cultural heritage, located on top of unstable rock masses lying on soft plastic bedrock is common. For example the cities of Agrigento (Ciampalini et al., 2012); San Leo (Borgatti et al., 2015; Frodella et al., 2016), Volterra (Pratesi et al., 2015; Bianchini et al., 2015), and Capri (Salvini et al., 2011) are affected by rockfalls and rockslides which involved part of their cultural heritage. The coupling between hard-brittle rocks located at the top of soft-plastic sediments is a framework which allow the generation of complex landslides. Rockfalls and rockslides usually affect the highest part of the reliefs, whereas the lowest part is affected by rotational and translational landslides (Varnes, 1978).

Several techniques can be used in order to detect subtle movements related to ground deformation of unstable rock masses. Most of these methods require for a dedicated ground based monitoring system such as Terrestrial Laser Scanner (Oppikofer et al., 2009; Kaperski et al., 2010), Ground Based SAR interferometer (Antonello et al., 2004; Gigli et al., 2011), GPS total station (Gaffet et al., 2009; Nishii & Matsuoka, 2010), extensometers and tiltmeters (Strouth et al., 2006) and seismic networks (Helmstetter & Garambois, 2010).

Usually all the aforementioned techniques are installed after a slope failure in order to monitor the stability of the slope and to evaluate the presence of residual ground deformation phenomena. Satellite multi-interferometric SAR data (for example data processed through the Permanent Scatterers SAR Interferometry, PSInSAR) are routinely used to evaluate ground deformation phenomena such as landslides and subsidence (Hanssen et al., 2005; Herrera et al., 2010; Raspini et al., 2014). This technique allows measuring ground displacements with millimeter accuracy exploiting archival data available since the 1992 (Ferretti et al., 2001; 2011). Time series analysis of deformation can be fruitfully used in order to detect unstable areas before the occurrence of an expected event and to study the evolution in time of a considered phenomenon. PSInSAR data are useful to detect, for example, precursory ground deforma-

(*) Dipartimento di Scienze della Terra, University of Florence.

tion phenomena which can occur in an unstable area where no important slope failures have not happened yet.

We present the outcomes of several Advanced InSAR analysis for the small village of Naso, in the Messina Province (Sicily). Naso is historically affected by slope instability phenomena. Between January and February 2010 an exceptional rainfall period affected the Nebrodi Mountains causing several slope failure phenomena (Caronia, San Fratello, Castell'Umberto, Sant'Angelo di Brolo and many others) (Bardi et al., 2014; Ciampalini et al., 2014; 2015). The most common hillslope processes were represented by complex, rotational and translational landslides. Naso, for its peculiar geological framework, has been affected also by rockfalls phenomena. PSInSAR analysis has been performed for this test site in order to detect precursory phenomena between 1992 and 2009 and to evaluate the presence of residual movements after the 2010 event.

2. STUDY AREA

Naso is a small village founded during the middle age with about 4,000 inhabitant. Its cultural heritage is represented by historical baroque churches. Naso is located in the northeastern sector of Sicily (Italy), along the Tyrrhenian coastline (Figure 1) within the Nebrodi Mountain range.

The village is placed on an N-S oriented divide which separate the main course of the Naso stream from its affluent, the Mancogna stream. The altitude of the eastern slope varies between 40 and 497 m asl, whereas the western slope is characterized by a reduced difference in height: from 400 to 497 m asl. Most of the hillslope processes developed along the eastern slope where several complex landslides and rockfalls are mapped by the official landslide inventory of the PAI (Hydrogeological Setting Plane) of the Sicily Region (Figure 1). Usually, rockfalls phenomena are located in the upper part of the slope. Most of the landslides mapped in the PAI are today active confirming that Naso is an unstable area with a very high landslide risk.

From a geological point of view, Naso is located on the top of a hill constituted by the Pleistocene in age calcareous sandstones of the "Calcareni di San Corrado" formation which are made of an alternation of calcareous sandstones and unconsolidated sands (Carmisciano et al., 1981; Antonioli et al., 2006). These sandstones, about 130 m thick, lies on 15 m of polygenic conglomerates which includes centimetric layers of sands rich in bioclasts. The Pleistocene deposits lies in unconformity on the Capo d'Orlando Flysch which, in this area, is made of arenites with clayey levels. The deposition of the Capo d'Orlando Flysch occurred between the Upper Oligocene and the Lower Burdigalian. The aforementioned deposits lies on a substrate formed by metabasites (gneiss and amphibolites) belonging to the Aspromonte Unit.

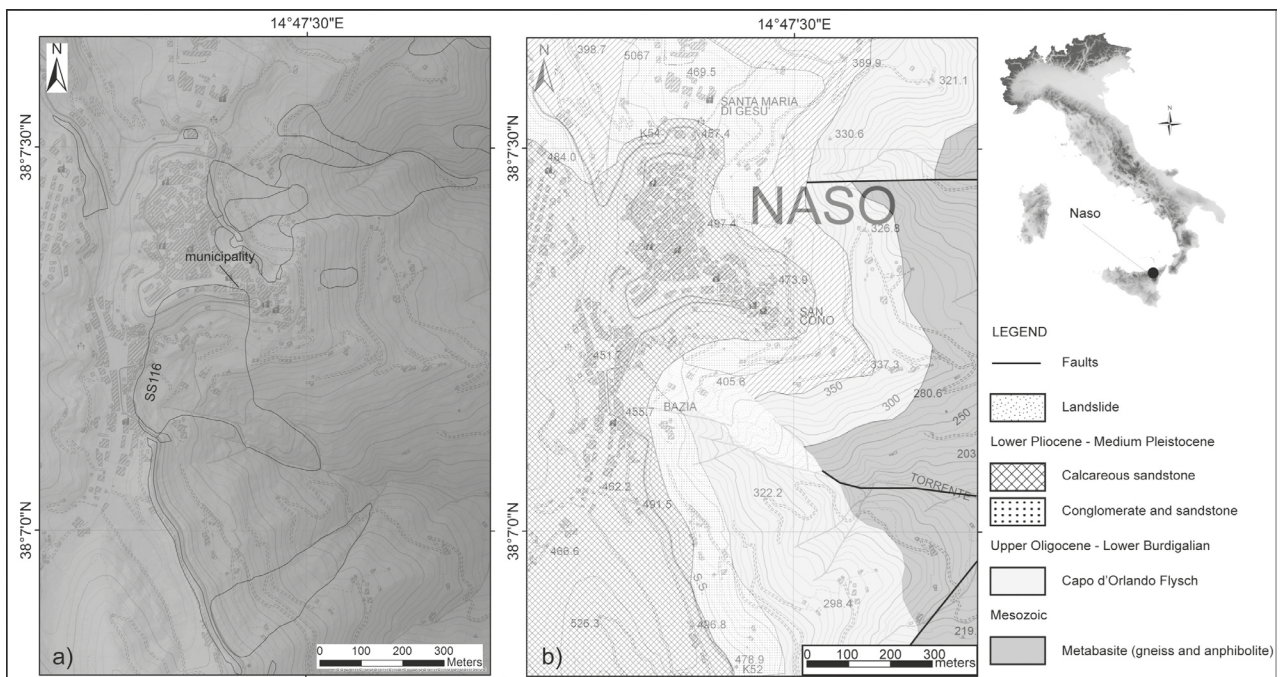


Figure 1 - Location of the study area: a) hillshade of the study area, black lines represents the PAI (Hydrogeological Setting Plane) landslide boundaries; b) geological map of the study area.

3. METHODOLOGY

Phase information of SAR images obtained by space borne sensors can be exploited through the conventional Differential SAR Interferometry (DInSAR), a method designed to retrieve, along the Line Of Sight (LOS) of the satellite, ground displacement occurred between the two different acquisitions of the same area (Gabriel et al., 1989; Massonnet and Feigl, 1998). The possibility of retrieving ground deformations that may have occurred between the first and the second acquisition is limited by different constraints, named temporal and geometrical decorrelation (Zebker and Villasenor, 1992) and by phase distortions introduced by atmospheric artifacts (Massonnet and Feigl, 1995). To overcome the main limitations of single-pair interferogram, different methods (under the “family name” Persistent Scatterer Interferometry, PSI), have been developed (e.g. Ferretti et al., 2000; Werner et al., 2003; Hooper et al., 2004; van der Kooij et al., 2006; Bianchini et al., 2013). Whatever the method, all these approaches rely on the phase analyses of multi-temporal stacks of satellite SAR images of the same target area. The main idea behind these methods is to identify pixels exhibiting good phase coherence over the entire observation period, via proper statistical analyses. Typically, at least 15 images should be available for carrying out a reliable PSI analysis (Colesanti and Wasowski, 2006). Of course, the larger the number of images the more precise and robust the results.

Within the first family, PSInSAR (Permanent Scatterer InSAR) (Ferretti et al., 2000, 2001) was the first technique specifically implemented for the processing of long stacks of SAR images. Signal analysis of a network of coherent radar targets (i.e. the Persistent Scatterers, PS), exhibiting high phase stability over the entire observation time period, allows estimating occurred displacement, acquisitions by acquisition. Following the PSInSAR approach many multi-interferometric techniques were developed and proposed, among which the SqueeSAR (Ferretti et al., 2011)

technique, capable of extending the ability of PSI to natural terrain (Raspini et al., 2013) through the detection of both point-wise coherent scatterers (i.e. the PS) and partially coherent Distributed Scatterers (DS). DS correspond to groups of pixels sharing similar radar returns.

Exploitation of output products of a PSI analysis, both average deformation rates and displacement time series, revealed valuable information for the study area. Unlike the DInSAR approach, PSI analysis is designed to generate time-series of ground deformations for individual elementary reflectors, assuming a linear model of deformation (Ferretti et al., 2001; Werner et al., 2003), or exploiting algorithms estimating the linear and nonlinear components of the displacement (e.g. Mora et al., 2003). The accuracy of the single measurement in correspondence of each SAR acquisition ranges from 1 to 3 mm (Colesanti et al., 2003). Each measurement is referred temporally and spatially to a unique reference image and to a stable reference point.

Besides deformation rates maps, SqueeSAR analysis for the processed datasets provides also, for each measurement point, a time series of deformation, which describes the evolution of displacement over the entire period. Each measurement of the time series corresponds to a single satellite acquisition. Time series shows the temporal pattern of the deformation, highlighting non-linear movements, seasonal trends, ground acceleration and any potential changes occurred during the analyzed period. Points are located in the most critical areas, i.e., the areas characterized by the highest deformation velocities, and have been selected to identify the presence of potentially precursor movements and to evaluate changes in deformation rates. The potential of repeat-pass space-borne SAR interferometry can be exploited not only to map the extension of affected areas but also to evaluate their deformation history. Displacement time series available for each PS in the area of interest are ideally suited for studying temporally continuous geohazard-related ground motions.

Table 1 - Description of the available SAR data.

Satellite	Geometry	Acquisition period	Available images	Track
ERS1/2	Ascending	11/09/1992 – 05/06/2000	34	129
ERS1/2	Descending	01/05/1992 – 08/01/2001	70	494
ENVISAT	Ascending	22/01/2003 – 22/09/2010	65	129
ENVISAT	Descending	07/07/2003-13/09/2010	49	494
RADARSAT-1	Ascending	31/01/2006-03/02/2010	47	104
RADARSAT-1	Descending	31/01/2006-03/02/2010	47	211
COSMO-SkyMed	Ascending	01/05/2011-03/05/2012	32	224
COSMO-SkyMed	Descending	16/05/2011-02/05/2012	32	98
TerraSAR-X	Descending	28/02/2011-22/09/2012	30	17

In this study SAR data acquired between 1992 and 2012 were used to detect the presence of precursory phenomena and to evaluate the residual movements with respect to the 2010 event of the area close to the village of Naso. All the investigated dataset were processed by using the SqueeSAR technique. The used data are reported in Table 1.

The time series analysis has been performed following the approach described in Cigna et al. (2011), under-sampling the whole time interval of observation into different sub-samples. For each sub-sample the deformation rate has been evaluated using a simple linear regression.

4. RESULTS

Results obtained by using ERS 1/2 data suggest an overall stability of the village during their acquisition period (1992-2001). Ground deformation can be recognized along the southern side of the village (sector 2 in Figure 2a) in correspondence with the main road (SS116) and the municipality (sector 1 in Figure 2a). Two PS of the ascending dataset, characterized by the highest velocity, are located inside an active landslide mapped in the PAI (Figure 2). The northern one (sector 1 in Figure 2) shows a ground deformation velocity of -1.79 mm/yr measured along the LOS. The detected velocity is close to the stability threshold (± 1.5 mm/yr) but it is located in correspondence with the main the area affected by the 2010 rockfall. The stability threshold was decided on the basis of the standard deviation of the velocity for each dataset, considering as stable the 90% of the PS population (Notti et al., 2014). The second PS (sector 2 in Figure 2a) is located along the SS116 and shows the highest velocity (-4.45 mm/yr). Also this point is placed along the main scarp of the landslide mapped in the PAI confirming that this sector was active between 1992 and 2001. The descending dataset (Figure 2b) confirms the instability of the southern side of Naso, in this case a single PS (sector 3 in Figure 2b) shows a velocity of -5.19 mm/yr. The PS is located outside the boundary of the PAI landslide suggesting that this phenomena can be wider than expected. The analysis of the time series (Figure 2) of the moving points do not shows the presence of acceleration periods. The deformation is characterized by a linear trend.

The presence of instability phenomena which affect the southern slope of Naso is confirmed by the ENVISAT data acquired between 2003 and 2010. The longer acquisition period of ENVISAT, with respect to ERS, allowed to increase the PS density. All the moving PS detected in the ascending geometry (Figure 3a) are located inside the landslide mapped on the southern slope of NASO in the PAI landslide inventory map.

The maximum recorded ground deformation velocity in this sector is -3.10 mm/yr along the SS116 (sector 2 in Figure 3a) and close to the municipality (sector 1 in Figure 3a). These results confirm that the southern slope of Naso was affected by subtle movements in a long period before the main event occurred in the 2010. The descending dataset (Figure 3b) does not highlight the presence of ground deformation.

The analysis of the time series (Figure 3c and 3d) highlights the presence of possible acceleration periods during the 2006 and the 2007 when the linear behavior of the deformation changes abruptly.

Radarsat-1 data are characterized by a higher PS density with respect to the ERS and ENVISAT ones. The acquisition period of Radarsat-1 data partially overlaps those of ENVISAT and clearly highlights the ground deformation which affects the southern slope of Naso. In particular the area close to the municipality (sector 1 in Figure 4) is characterized by an average ground deformation velocity of -3.05 mm/yr. The highest velocities (-5.88 mm/yr) were detected along the SS116 (sector 2 in Figure 4). Furthermore, thanks to the ascending dataset (Figure 4a) was possible to detect an area, located within the eastern slope of Naso, affected by ground deformation phenomena (sector 3 in Figure 4). Here the registered average velocity is -3.00 mm/yr. The descending dataset (Figure 4b) substantially confirms the deformation of the southern slope of Naso. The time series analysis (Figure 4), especially those of the ascending dataset shows the presence of two periods of acceleration: the first one between August and October 2008 and the second one between April and July 2009.

COSMOSky-Med (CSK) data were acquired between the 2011 and the 2012 in order to evaluate the presence of residual movement after the 2010 event. The obtained results highlight the presence of residual movements within the southern slopes (Figure 5). The area close to the municipality (sector 1 in Figure 5a) is still affected by ground deformation. The municipality and several others buildings have been evacuated at the beginning of the 2014 after the development of centimetric cracks and fissures on the facades of the buildings. The ground deformation velocities measured in this area by CSK ranges between -4.1 mm/yr and -13.2 mm/yr confirming the high risk related to this area. The highest velocities (up to -21.9 mm/yr) were detected along the SS116 (sector 2 in Figure 5a), where important stabilization measures have been planned in order to avoid the interruption of the road. Despite the descending dataset (Figure 5b) is less informative, it confirms the presence of ground deformation phenomena in correspondence with the municipality. Time series analysis (Figure 5c) highlights that the deformation is continuous and fast (about 20 mm in one year). In particular the ground deformation

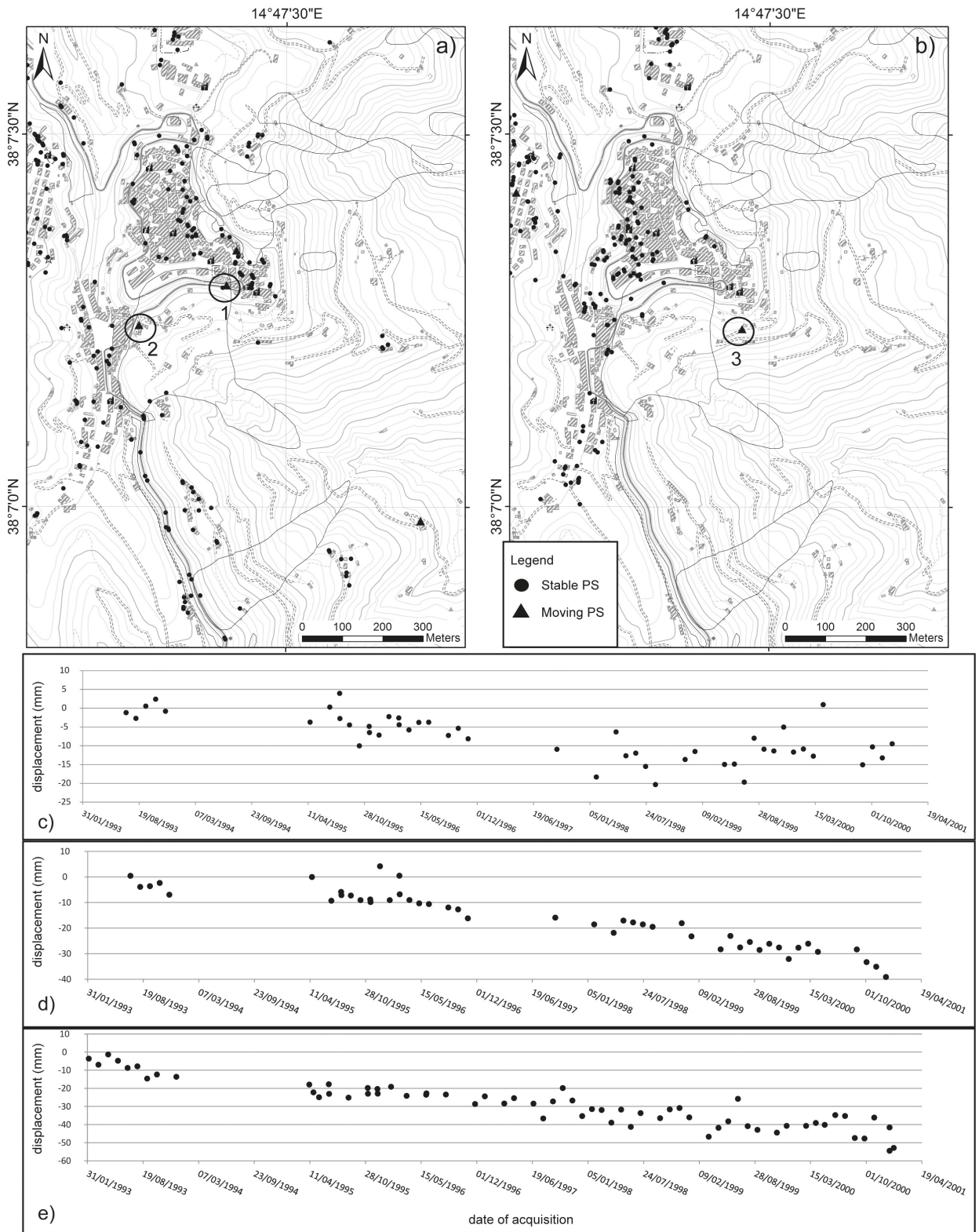


Figure 2 - Ground deformation map obtained by using the ERS 1/2 ascending (a) and descending (b) datasets. Example of three time series of cumulative displacement extracted from PS: c) corresponds to the time series extracted from point 1 in Figure 2a; d) corresponds to the time series extracted from point 2 in Figure 2a; e) corresponds to the time series extracted from point 3 in Figure 2b.

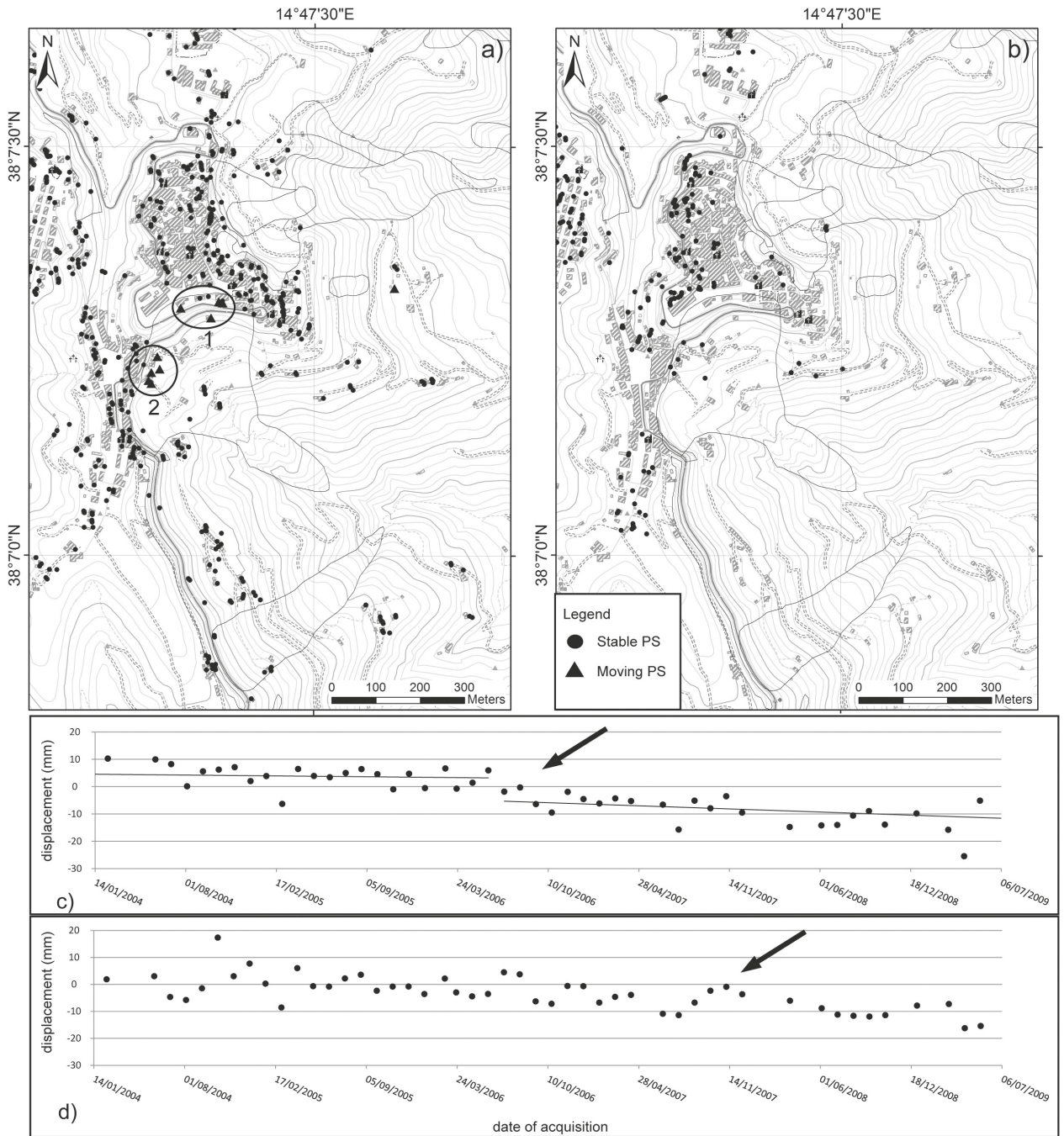


Figure 3 - Ground deformation map obtained by using the ENVISAT ascending (a) and descending (b) datasets. Example of two time series of cumulative displacement extracted from PS: c) corresponds to the time series extracted from point 1 in Figure 3a; d) corresponds to the time series extracted from point 2 in Figure 3a. The black arrows highlight two periods of acceleration.

detected between the 2011 and 2012 seems to be localized only within the southern slopes. No evidences of deformation have been recognized along the eastern slope despite the presence of landslides as reported in the PAI.

In order to validate the CSK data between the 2011 and the 2012, TerraSAR-X (TSX) data were acquired and compared. In this case only the descending dataset (Figure 6a) was available. TSX data substantially confirm the results obtained by using CSK. The southern

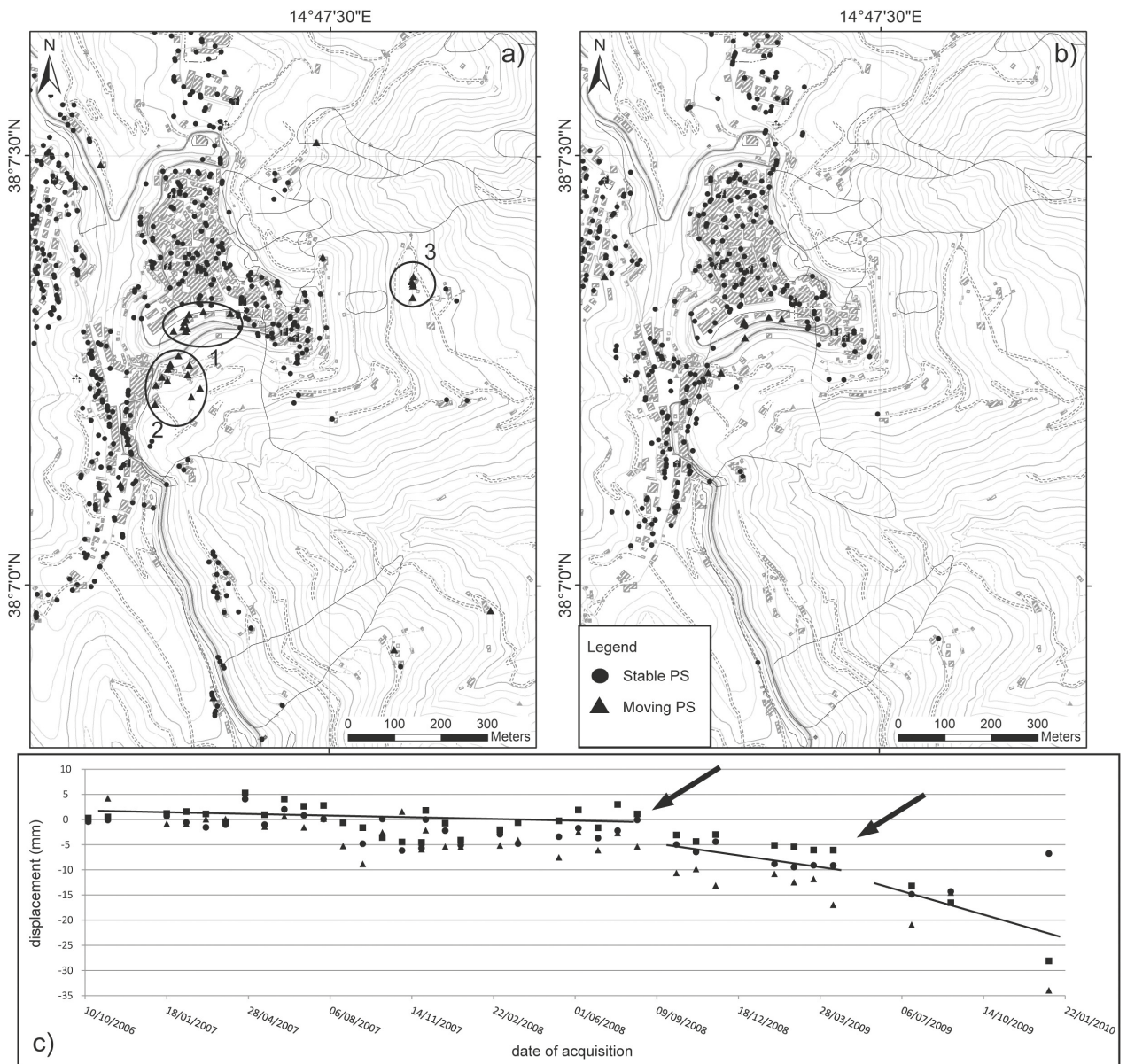


Figure 4 - Ground deformation map obtained by using the Radarsat-1 ascending (a) and descending (b) datasets. c) Example of three time series of cumulative displacement extracted from PS located inside the sector 1 in Figure 4a.

sector is affected by ground deformation phenomena having a maximum velocity around -22 mm/yr. Both the area close to municipality (sector 1 in Figure 6a) and the area located along the SS116, south of Naso (sector 2 Figure 6a) show PS characterized by high velocity (between -15 and -22 mm/yr). The rest of the village appears as stable. Time series analysis confirms the general linear and continuous trend of the deformation during the acquisition period (Figure 6b). The more regular acquisition in time makes TSX time series more reliable with respect to those obtained with CSK.

5. DISCUSSION

In order to understand the triggering factors of the slope instability processes that affect the village of Naso, the time series of moving PS have been compared to the rainfall data available from the 2002 for the Naso measuring station and to the seismic activity of the area. The comparison can not be performed for the ESR 1/2 dataset because this satellite ended to acquire images in the 2001 and the rainfall data are available from the 2002. The analysed ENVISAT

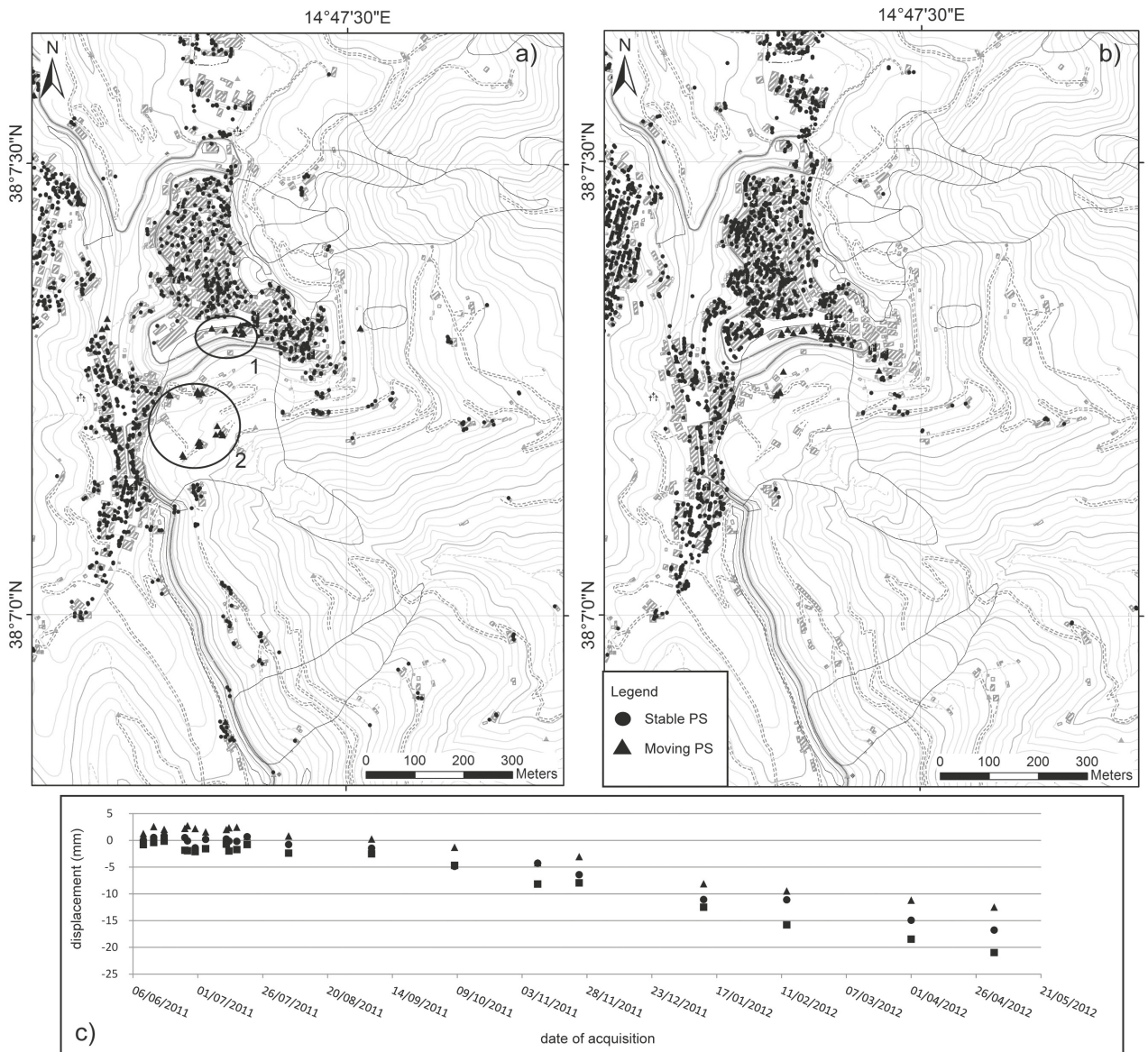


Figure 5 - Ground deformation map obtained by using the COSMO-SkyMed ascending (a) and descending (b) datasets. c) Example of three time series of cumulative displacement extracted from PS located inside the sector 1 in Figure 5a.

time series show an overall stability between the 2003 and July 2006 (Figure 7). Starting from August 2006 an abrupt increase of the deformation velocity can be detected (from 0.02 mm/d to 0.24 mm/d). This period was characterized by both an increase of the rainfall with three peaks greater than 60 mm/m and by the presence of two earthquakes having a magnitude greater than 3 Mw (3.2 and 3.3). Considering the rest of the period covered by ENVISAT it can be noted that rainfall events represent the main triggering factor of the increase of the deformation velocity (Figure 7).

In particular, each time that the monthly rainfall exceed 60 mm the time series show an increase of the displacement.

A similar correlation can be observed considering the RADARSAT-1 data when they are compared to rainfall and seismicity data. Increases of the deformation velocity can be observed in correspondence of rainfall events characterized by a monthly precipitation greater than 60 mm (Figure 8). In this case RADARSAT-1 times series seem to record the 1st of May 2009 earthquake (3 Mw) better than ENVISAT. The different

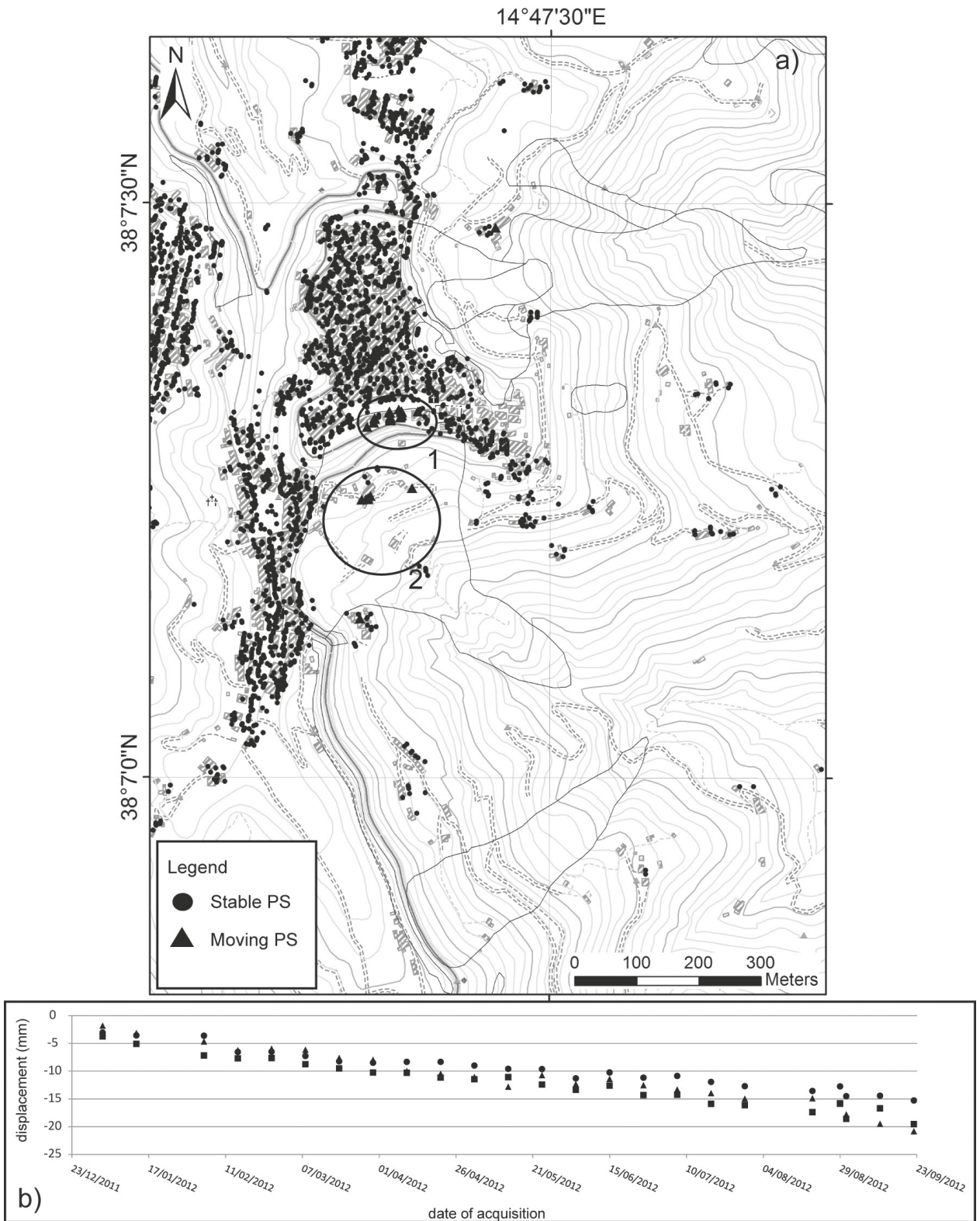


Figure 6 - a) Ground deformation map obtained by using the TerraSAR-X descending datasets. b) Example of three time series of cumulative displacement extracted from PS located inside the sector 1 in Figure 6a.

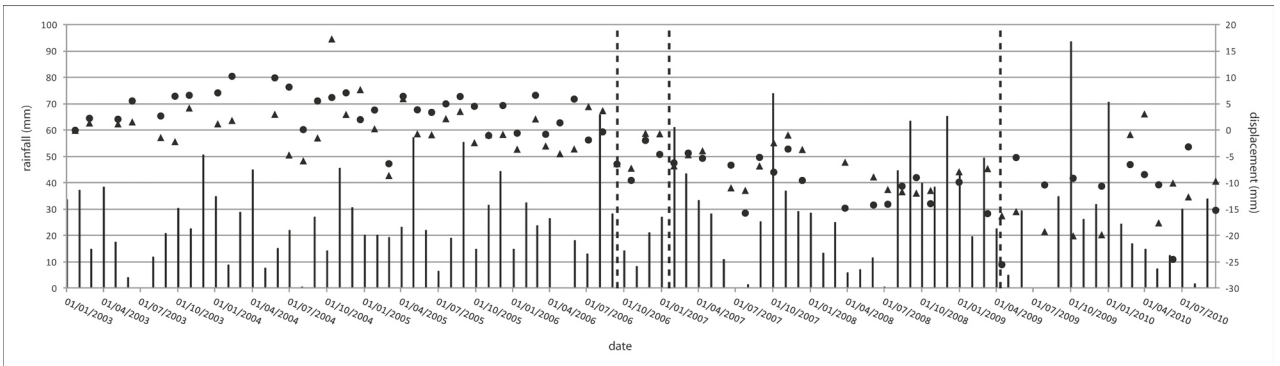


Figure 7 - Comparison between the ENVISAT time series of cumulative displacement, the monthly rainfall data and the earthquakes greater than 3 Mw (dashed lines).

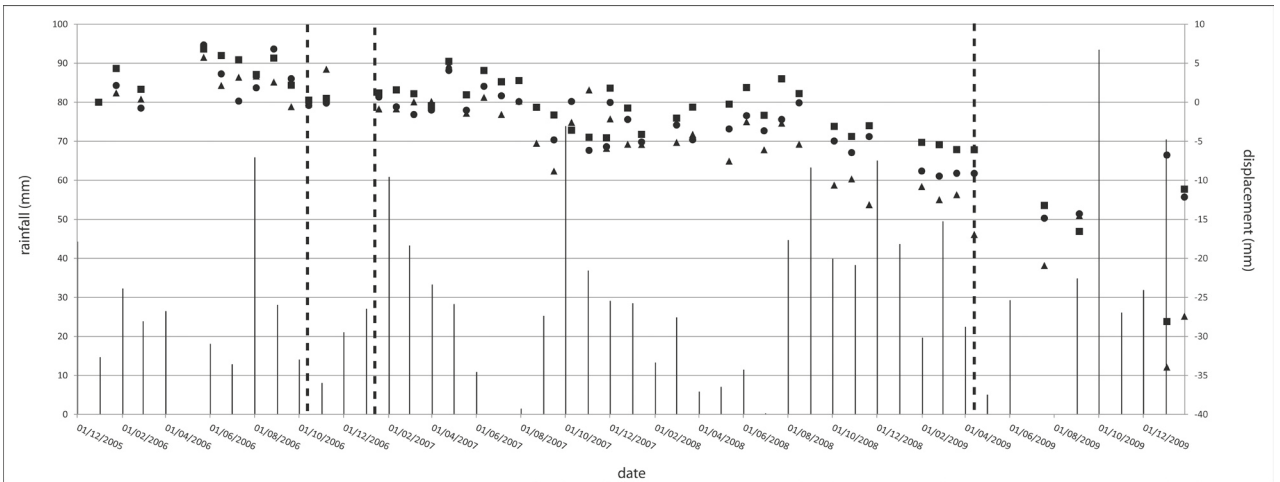


Figure 8 - Comparison between the RADARSAT-1 time series of cumulative displacement, the monthly rainfall data and the earthquakes greater than 3 Mw (dashed lines).

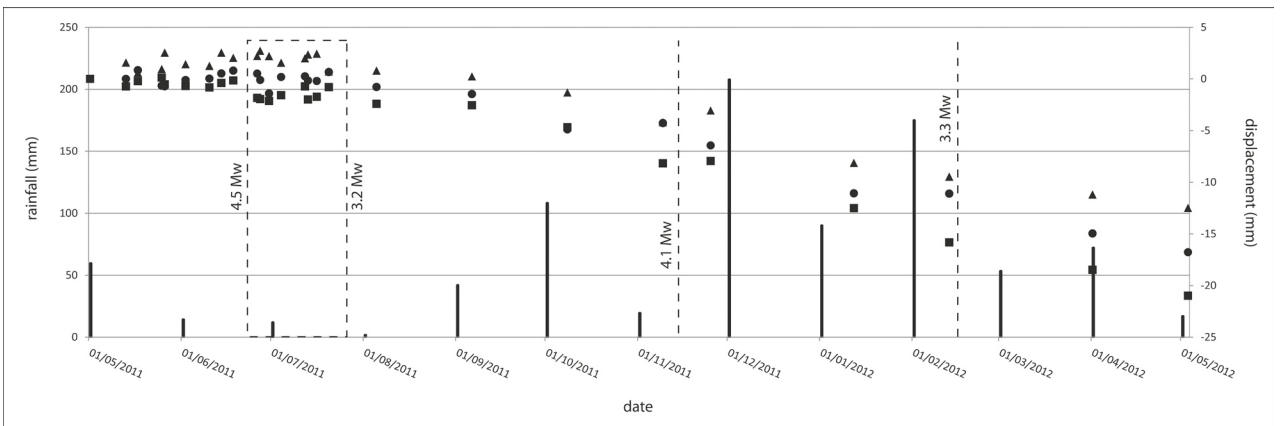


Figure 9 - Comparison between the COSMO-SkyMed time series of cumulative displacement, the monthly rainfall data and the earthquakes greater than 3 Mw (dashed lines) The dashed rectangle indicates the earthquake swarm (23/06/2011 – 27/07/2011).

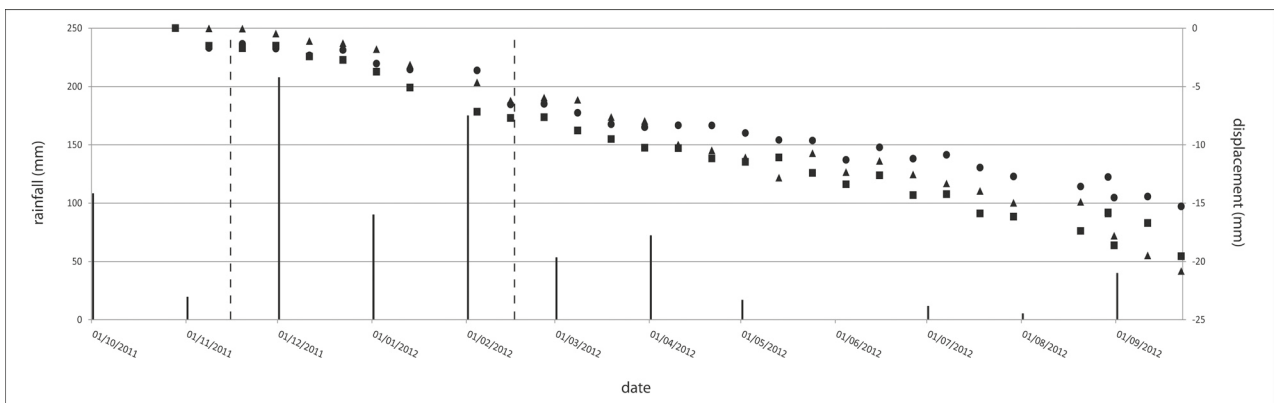


Figure 10 - Comparison between the TerraSAR-X time series of cumulative displacement, the monthly rainfall data and the earthquakes greater than 3 Mw (dashed lines) The dashed rectangle indicates the earthquake swarm (23/06/2011 – 27/07/2011).

slopes of the time series as reported in figure 4 suggest that rainfall events trigger the observed increase in the deformation.

The correlation between the deformation pattern and the rainfall data is confirmed also by COSMO-SkyMed data (Figure 9). In this case the increase of the displacement follows an earthquake swarm occurred between 23rd June 2006 and the 27th July 2006 represented by seven earthquakes with magnitude between 3.0 and 4.5 Mw. A further increase of the deformation can be observed from October 2011 when rainfall exceed 60 mm/month.

TerraSAR-X data ranges between October 2011 and December 2012. The first months of acquisition period shows an increase of the deformation which corresponds to the wetter period, between October 2011 and April 2012 five months exceed 60 mm/m of rainfall (Figure 10). From April 2012 the deformation trend continues despite monthly rainfall strongly decrease. This persistence of the deformation trend can be related to the exceptional rainfall occurred during the previous months (up to 207 mm/m in December 2011 and up to 175 mm/m in February 2012).

Time series analysis is very suitable to investigate the long term evolution of the deformation of a selected area. In particular these kind of data can be compared to the temporal occurrence of specific triggering factors (rainfall, earthquakes) in order to detect which is the most important factor that cause landslides. In this case a rainfall threshold has been detected (60 mm/m). Despite the advantages of the PSInSAR technique it is not possible, today, use it as monitoring system in order to predict future landslides. This problem is related to the acquisition period, which varies between 16 and 35 days. This period of time does not allow to promptly update of the time series in order to understand their future evolution. Periods of increase of the deformation velocity can be

detected considering multiple acquisitions. PSInSAR can be profitably used in combination with other techniques able to detect ground deformation in a reduced period of time (GB-InSAR), in this case PSInSAR integrates the information obtained through other systems allowing for a very complete back monitoring of the ground deformation phenomena. PSInSAR technique is useful to detect areas affected by ground deformation where triggering factors can cause landslides but it is not possible to use it as a real time monitoring system.

6. CONCLUSIONS

This work highlights the usefulness of the satellite A-DInSAR based deformation time series to detect, monitor and forecast landslide phenomena. The very long temporal period (about 20 years) of observation can be fruitfully used to detect precursory phenomena, considering a well known landslide event and to evaluate the presence of residual movement that can be considered precursory phenomena with respect to the possible re-activation of future slope failure. This methodology was tested in the small village of Naso which is historically affected by landslides. During the 2010 several important landslides damaged the village. SAR data were acquired since the 1992 to the 2010 event. These data clearly show that the southern sector was affected by ground deformation characterized by periods of acceleration that can represent precursory phenomena of the 2010 landslides. SAR data were used also to evaluate the residual movement after the 2010 phenomena. These data highlight that the village still suffers from problems related to slope instability phenomena characterized by an average velocity greater than those measured before the 2010. The obtained results high-

lights how this technique can be successfully used at local scale to monitor and forecast hillslope processes. The space borne monitoring system must not be considered as a real time system but as a system able to monitor the long term evolution of slope instability phenomena which can be related to specific triggering factors. The time series trends can be used to establish rainfall thresholds that can be used to predict the landslide occurrence in case of specific rainfall events.

ACKNOWLEDGEMENTS

This research was founded by PRIN PROJECT 2010–2011 “Time-space prediction of high impact landslides under changing precipitation regimes”. The research leading to these results received also funding from the European Union Seventh Framework Program (FP7/2007–2013) under grant agreement No. 242212 (Project DORIS). PSI data were processed by Tele-Rilevamento Europa. We thanks the “Servizio Informativo Agrometeorologico Siciliano” for the rainfall data and an anonymous reviewer for the helping suggestions.

REFERENCES

- ANTONELLO G., CASAGLI N., FARINA P., LEVA D., NIO G., SIEBER A.J., TARCHI D., 2004. Ground-based SAR interferometry for monitoring mass movements. *Landslides* 1: 21-28.
- ANTONIOLI F., FERRANTI L., LAMBECK K., KERSHAW S., VERRUBBI V., DAI PRA G., 2006. Late Pleistocene to Holocene record of changing uplift rates in southern Calabria and northeastern Sicily (southern Italy, Central Mediterranean Sea). *Tectonophysics* 422: 23-40.
- BARDI F., FRODELLA W., CIAMPALINI A., BIANCHINI S., DEL VENTISETTE C., GIGLI G., FANTI R., MORETTI S., BASILE G., CASAGLI N., 2014. Integration between ground based and satellite SAR data in landslide mapping: The San Fratello case study. *Geomorphology* 223: 45-60.
- BIANCHINI S., HERRERA G., MATEOS R.M., NOTTI D., GARCIA I., MORA O., MORETTI S., 2013. Landslide activity maps generation by means of persistent scatterer interferometry. *Remote Sensing* 5(12): 6198-6222.
- BIANCHINI S., PRATESI F., NOLESINI T., CASAGLI N., 2015. Building damage assessment by means of PSI (Persistent Scatterer Interferometry) analysis 1 on a landslide-affected area: the Volterra (Italy) case study. *Remote Sensing* 7: 4678-4701.
- BORGATTI L., GUERRA C., NESCI O., ROMEO R.W., VENERI F., LANDUZZI A., BENEDETTI G., MARCHI G., LUCENTE C.C., 2015. The 27 February 2014 San Leo landslide (northern Italy). *Landslides* 12: 387-394.
- CARMISCIANO R., GALLO L., LANZAFAME G., PUGLISI D., 1981. Le calcareniti di Floresta nella costruzione dell'Appennino Calabro-Peloritano (Calabria e Sicilia). *Geologica Romana* 20: 171-182.
- CIAMPALINI A., CIGNA F., DEL VENTISETTE C., MORETTI S., LIGUORI V., CASAGLI N., 2012. Integrated geomorphological mapping in the north-western sector of Agrigento (Italy). *Journal of Maps* 8: 136-145.
- CIAMPALINI A., BARDI F., BIANCHINI S., FRODELLA W., DEL VENTISETTE C., MORETTI S., CASAGLI N., 2014. Analysis of building deformation in landslide area using multisensor PSInSAR technique. *International Journal of Applied Earth Observation and Geoinformation* 33: 166-180.
- CIAMPALINI A., RASPINI F., BIANCHINI S., FRODELLA W., BARDI F., LAGOMARSINO D., DI TRAGLIA F., MORETTI S., PROIETTI C., PAGLIARA P., ONORI R., CORAZZA A., DURO A., BASILE G., CASAGLI N., 2015. Remote sensing as tool for development of landslide databases: The case of the Messina Province (Italy) geodatabase. *Geomorphology* 249: 103-118.
- CIGNA F., DEL VENTISETTE C., LIGUORI V., CASAGLI N., 2011. Advanced radar-interpretation of InSAR time series for mapping and characterization of geological processes. *Natural Hazards and Earth System Sciences* 11: 865-881.
- COLESANTI C., FERRETTI A., PRATI C., ROCCA F., 2003. Monitoring landslides and tectonic motions with the Permanent Scatterers Technique. *Engineering Geology* 68(1): 3-14.
- COLESANTI C. AND WASOWSKI J., 2006. Investigating landslides with space-borne Synthetic Aperture Radar (SAR) interferometry. *Engineering Geology* 88: 173-199.
- FERRETTI A., PRATI C., ROCCA F., 2000. Nonlinear subsidence rate estimation using permanent scatterers in differential SAR interferometry. *Geoscience and Remote Sensing, IEEE transactions on* 38(5): 2202-2212.
- FERRETTI A., PRATI C., ROCCA F. 2001. Permanent scatterers in SAR interferometry. *Transactions on Geoscience and Remote Sensing, IEEE* 39(1): 8-20.
- FERRETTI A., FUMAGALLI A., NOVALI F., PRATI C., ROCCA F., RUCCI A., 2011. A new Algorithm for Processing Interferometric Data-Stacks: SqueeSAR. *IEEE Transaction on Geoscience and Remote Sensing* 49(9): 3460-3470.
- FRODELLA W., CIAMPALINI A., GIGLI G., LOMBARDI L., RASPINI F., NOCENTINI M., SCARDIGLI C., CASAGLI N., 2016. Synergic use of satellite and ground based remote sensing methods for the San Leo rock cliff monitoring. *Geomorphology*, (in press).
- GABRIEL A.K., GOLDSTEIN R.M., ZEBKER H.A., 1989. Mapping small elevation changes over large areas: differential radar interferometry. *Journal of Geophysical Research: Solid Earth*, 94(B7): 9183-9191.
- GAFFET S., GUGLIELMINI Y., CAPPÀ F., PAMBRUN C., MONFRET T., AMITRANO D., 2009. Use of the simultaneous seismic, GPS and meteorological monitoring for the characterization of a large unstable mountain slope in the southern French Alps. *Geophysical Journal International* 182: 1395-1410.
- GIGLI G., FANTI R., CANUTI P., CASAGLI N., 2011. Integration of advanced monitoring and numerical modeling techniques for the complete risk scenario analysis of rockslides: The case of Mt. Beni (Florence, Italy). *Engineering Geology* 120: 48-59.
- HANSEN R.S., 2005. Satellite radar interferometry for deformation monitoring: a priori assessment of feasibility and accuracy. *International Journal of Applied Earth Observation Geoinformation* 6: 253-260.
- HELMSTETTER A., GARAMBOIS S., 2010. Seismic monitoring of Séchilienne rockslide (French Alps): Analysis of seismic signals and their correlation with rainfalls. *Journal of Geophysical Research* 115: F03016.

- HERRERA G., TÓMAS R., MONELLS D., CENTOLANZA G., MALLORQUI J.J., VICENTE F., NAVARRO V.D., LOPEZ-SANCHEZ J.M., SANABRIA M., CANO M., MULAS J. 2010. Analysis of subsidence using TerraSAR-X data: Murcia case study. *Engineering Geology* 116: 284-295.
- HOOPER A., ZEBKER H., SEGALL P., KAMPES B. 2004. A new method for measuring deformation on volcanoes and other natural terrains using InSAR persistent scatterers. *Geophysical Research Letters* 31(23): L23611.
- KAPERSKI J., DELACOURT C., ALLMAND P., POTHERAT P., JAUD M., VARREL E., 2010. Application of a Terrestrial Laser Scanner (TLS) to the study of the Séchillienne Landslide (Isère, France). *Remote Sensing* 2: 2785-2802.
- MASSONNET D., FEIGL K.L., 1995. Discrimination of geophysical phenomena in satellite radar interferograms. *Geophysical Research Letters* 22(12): 1537-1540.
- MASSONNET D., FEIGL K.L., 1998. Radar interferometry and its application to changes in the Earth's surface. *Reviews of Geophysics* 36: 441-500.
- MORA O., MALLORQUI J.J., BROQUETAS A., 2003. Linear and nonlinear terrain deformation maps from a reduced set of interferometric SAR images. *Geoscience and Remote Sensing, IEEE Transactions on* 41(10): 2243-2253.
- NISHII R., MATSUOKA N., 2010. Monitoring rapid head scarp movement in an alpine rockslide. *Engineering Geology* 115: 49-57.
- NOTTI D., HERRERA G., BIANCHINI S., MEISINA C., GARCIA-DVALILLO J.C., ZUCCA F., 2014. A methodology for improving landslide PSI data analysis. *International Journal of Remote Sensing* 35: 2186-2214.
- OPPIKOFER T., JABOYEDOFF M., BLIKRA M., DERRON M. H., METZGER R., 2009. Characterization and monitoring of the Åknes rockslide using terrestrial laser scanning. *Natural Hazards and Earth System Sciences* 9: 1003-1019.
- PRATESI F., NOLESINI T., BIANCHINI S., LEVA D., LOMBARDI L., FANTI R., CASAGLI N., 2015. Early Warning GBInSAR-Based Method for Monitoring Volterra (Tuscany, Italy) City Walls. *IEEE Journal of Selected Topics in Applied Earth Observations and Remote Sensing* 8: 1753-1762.
- RASPINI F., MORETTI S., CASAGLI N., 2013. Landslide mapping using SqueeSAR data: Giampilieri (Italy) case study. In *Landslide Science and Practice* (pp. 147-154). Springer Berlin Heidelberg.
- RASPINI F., LOUPASAKIS K., ROZOS D., ADAM N., MORETTI S., 2014. Ground subsidence phenomena in the Delta municipality region (Northern Greece): Geotechnical modeling and validation with Persistent Scatterer Interferometry. *International Journal of Applied Earth Observation and Geoinformation* 28: 78-89.
- STROUTH A., BURK R.L., EBERHARDT E. 2006. The Afternoon Creek rockslide near Newhalem, Washington. *Landslides* 3: 175-179.
- SALVINI R., FRANCONI M., RICCUCCI S., FANTOZZI P.L., BONCIANI F., MANCINI S. (2011) Stability analysis of "Grotta delle Felci" Cliff (Capri Island, Italy): structural, engineering-geological. Photogrammetric surveys and laser scanning. *Bulletin of Engineering Geology and the Environment*, 70, 549-557.
- VAN DER KOOIJ M., HUGHES W., SATO S., PONCOS V. 2005. Coherent target monitoring at high spatial density: examples of validation results. In *Fringe Workshop*, European Space Agency.
- VARNES D.J. 1978. Slope movements and types and processes. In: *Landslides Analysis and Control*, Transportation Research Board Special Report 176:11-33
- WERNER C., WEGMÜLLER U., STROZZI T., WIESMANN A. 2003. Interferometric point target analysis for deformation mapping. In *Geoscience and Remote Sensing Symposium, 2003. IGARSS'03. Proceedings. 2003 IEEE International* (Vol. 7, pp. 4362-4364). IEEE.
- ZEBKER H., VILLASENOR J. 1992. Decorrelation in interferometric radar echoes. *Geoscience and Remote Sensing, IEEE Transactions on* 30(5): 950-959.

(ms. pres. 15 gennaio 2015; ult. bozze 3 ottobre 2016)

Edizioni ETS
Piazza Carrara, 16-19, I-56126 Pisa
info@edizioniets.com - www.edizioniets.com
Finito di stampare nel mese di giugno 2016

